Magnetically assisted trapping of passive colloids by active dipolar chain

A. Compagnie [1,2] N. Vandewalle [2] and E. Opsomer [2,*]
[1]*Institut für Theoretische Physik: Weiche Materie, Heinrich-Heine-Universität, D-40225 Düsseldorf, Germany*
[2]*GRASP, Institute of Physics B5a, University of Liège, B4000 Liège, Belgium*

(Received 7 October 2025; accepted 8 May 2026; published 27 May 2026)

We investigate a trapping mechanism for passive Brownian particles based on mixtures with self-propelled dipolar colloids. Active dipoles, whose magnetic moment is oriented perpendicularly to their propulsion direction, spontaneously form dynamic chains that collapse into clusters through dipole-dipole interactions. These transient structures efficiently capture nearby passive particles, forming dense phases at relatively low global packing fractions. Using Brownian dynamics simulations, we analyze how the capture efficiency depends on the Péclet number (Pe) and dipolar interaction strength (λ). We demonstrate that an external magnetic field, applied briefly to align the active dipoles, significantly enhances trapping efficiency, with capture fractions exceeding 50% under optimal conditions. Our results reveal a nontrivial competition between activity and dipolar forces, governed by the ratio λ/Pe, and offer insights into designing self-organized trapping strategies for passive colloids.

DOI: 10.1103/lfch-5drf

I. INTRODUCTION

Active systems, characterized by their ability to extract energy from their environment and convert it into motion [1], can self-organize into configurations that are unattainable in equilibrium conditions [2]. Originally observed in biological contexts [3–5], such behavior has since also been extensively investigated using artificial self-propelled particles, both experimentally [6–8] and through numerical and theoretical approaches [9–12]. One of the most striking collective phenomena emerging from activity is motility-induced phase separation (MIPS) [13]. While MIPS can arise solely from activity and steric interactions among spherical particles [14–16], the collective dynamics of the particles can be altered by considering additional features such as noncircular particles [17,18], phoretic interactions [19–21], local alignment [22–24], or self-alignment mechanisms [25,26].

Dipolar interactions between active colloids are of particular interest, due to the specific collective properties they can exhibit [27]. They may come from electrostatic imbalance, induced dipoles or permanent dipoles, collectively leading to a variety of possible configurations [28–32], such as chains, rings, or clusters. This can also be modified by tuning these interactions, for example, by shifting the position of the dipole [33], by having induced dipoles perpendicular to the self-propulsion [34], or by introducing additional traits such as chirality [35]. Another advantage of magnetic dipoles, in the optics of external control of active systems, is their response to external magnetic fields. This has been shown to have significant impact on the organization and the dynamics of the system [36,37].

Complex collective behaviors also stem from interaction between population of particles with varying characteristics, which will form mixtures [38]. This is already observed when considering simple differences, as in active-passive mixtures where MIPS occur with passive particles trapped in dense phases [39–43], but other effects may arise, such as the demixing of chiral active particles due to different chiral orientations [44,45]. By varying multiple characteristics, even more different collective phenomena may occur [27,46–50]. It is also possible to induce clustering of passive particles by observing active-passive mixtures and designing the active particles to be flexible and elongated, such as bucklebots [51] or wormlike structures [52].

This line of research is not only of fundamental interest but also relevant for practical applications. Inert contaminants, such as microplastics suspended in aqueous environments, can be effectively modeled as passive particles in a viscous medium. Developing self-organized strategies to trap such particles using active agents could open new avenues in solvent purification and environmental remediation [53,54]. However, activity alone is not always sufficient to achieve efficient trapping of passive components, particularly at the low concentrations required for spontaneous MIPS formation in mixed systems [40].

In this work, we investigate how dipolar interactions among active particles can assist in the formation of functional structures capable of efficiently capturing passive particles, even at low packing fractions. By characterizing the formation mechanisms, internal structure, and dynamics of these active-passive aggregates, we aim to identify robust and spontaneous trapping strategies.

The remainder of the paper is organized as follows. Section II introduces the model and key parameters used in the

*Contact author: eric.opsomer@uliege.be

simulations. In Sec. III, we present the trapping results under various conditions, with the aim of optimizing capture efficiency. Section IV offers a detailed analysis of how activity and dipole-dipole interactions shape the observed dynamics. Finally, Sec. V summarizes the main findings and discusses potential future directions.

II. MODEL

Our system consists in N colloids that we model as disks of diameter σ that are placed randomly in a fluid bath of viscosity η. These colloids form two separate populations because of their differing properties; N_a colloids are active Brownian particles with a central magnetic dipole, and N_p colloids are passive Brownian particles. Due to their characteristics, active disks are called active dipoles. Providing that inertial effects can be neglected, the system dynamics can be described by the following stochastic differential equations:

$$\dot{\mathbf{r}}_i = v_i \hat{\mathbf{n}}_i + \sqrt{2D_T}\,\boldsymbol{\xi}_T - \frac{\nabla_i U(\mathbf{r}_i,\theta_i)}{3\pi\eta\sigma}, \tag{1}$$

$$\dot{\theta}_i = \sqrt{2D_R}\,\xi_R - \frac{\partial_{\theta_i} U(\mathbf{r}_i,\theta_i)}{\pi\eta\sigma^3} + \frac{M_{B,i}}{\pi\eta\sigma^3}, \tag{2}$$

where $\boldsymbol{r}_i$ is the disk's position, θ_i its orientation with $\hat{\mathbf{n}}_i = (\cos\theta_i, \sin\theta_i)^T$, and v_i its self-propulsion velocity with $v_i = v_0$ for active dipoles and $v_i = 0$ for passive colloids. Parameters D_T and D_R denote the translational and rotational diffusion coefficients, respectively, and $\boldsymbol{\xi}_T$ and ξ_R correspond to Gaussian white noises with unit variance and zero mean. The persistence time is therefore defined as $\tau = 1/D_R$. The interaction potential $U(\mathbf{r}_i,\theta_i)$ is given by

$$U(\mathbf{r}_i,\theta_i) = \sum_{j\neq i}^{N} \big(u_{\mathrm{WCA}}(|\mathbf{r}_{ij}|) + u_{dd}(\mathbf{r}_{ij},\theta_i,\theta_j)\big), \tag{3}$$

with $\mathbf{r}_{ij} = \mathbf{r}_i - \mathbf{r}_j$. The first term corresponds to the short-ranged and repulsive Weeks-Chandler-Andersen (WCA) potential,

$$u_{\mathrm{WCA}}(r_{ij}) = \begin{cases} 4\epsilon\left(\left(\frac{\sigma}{r_{ij}}\right)^{12} + \left(\frac{\sigma}{r_{ij}}\right)^{6}\right) + \epsilon & \text{if } r_{ij} < 2^{1/6}\sigma \\ 0 & \text{otherwise} \end{cases} \tag{4}$$

with ϵ the energy scale of the contacts. The second term corresponds to the magnetic dipole-dipole interaction,

$$u_{dd}(\mathbf{r}_{ij},\theta_i,\theta_j) = \frac{\mu_0}{4\pi}\frac{\boldsymbol{\mu}_i\cdot\boldsymbol{\mu}_j - 3(\boldsymbol{\mu}_i\cdot\hat{\mathbf{r}}_{ij})(\boldsymbol{\mu}_j\cdot\hat{\mathbf{r}}_{ij})}{r_{ij}^3} \tag{5}$$

$$\boldsymbol{\mu}_i = \mu_i(\cos(\theta_i+\delta_i), \sin(\theta_i+\delta_i))^T, \tag{6}$$

where μ_0 is the vacuum permeability, μ_i the magnetic dipole moment with $\mu_i = \mu$ for active dipoles and $\mu_i = 0$ for passive colloids, and δ_i is the angle between $\boldsymbol{\mu}_i$ and $\hat{\mathbf{n}}_i$ which will be fixed to 0 or to $\pi/2$. An external magnetic field $\mathbf{B}$ may also be applied to the entire system. The corresponding magnetic torque exerted on the dipoles (and thus the disks) is given by

$$M_{B,i} = -\boldsymbol{\mu}_i\cdot\mathbf{B}. \tag{7}$$

The intensity of the external magnetic field can also be expressed by the adimensional number $B' = \sqrt{4\pi\sigma^3/\mu_0 k_B T}\,B$.

The global dynamics of the system will be mainly determined by the activity and the dipole-dipole interactions. Therefore, the Péclet number Pe and the magnetic dipolar adimensional number λ are relevant to estimate the behavior of the system. They are defined as

$$\mathrm{Pe} = \frac{2v_0}{\sigma D_r}, \tag{8}$$

$$\lambda = \frac{\mu_0}{4\pi}\frac{\mu^2}{\sigma^3 k_B T} \tag{9}$$

with the different parameters chosen from the active population of colloids.

III. RESULTS

A. Numerical simulations

Brownian dynamics simulations, using the Euler-Maruyama method implemented in our own C++ code, were conducted to investigate this model. The random Gaussian white noise was generated by a permuted congruential generator algorithm, using the C++ implementation from the PCG library [55]. A total of $N_a = 1000$ active dipoles and $N_p = 1000$ passive colloids are randomly placed in a 2D squared box of length $L = 125\sigma$ before the dynamics are evaluated with periodic boundary conditions. Each population constantly has a packing fraction ϕ of 0.05, defined as $\phi_i = N_i\pi\sigma^2/4L^2$. The dipoles have their orientation shifted by $\pi/2$ compared to the direction of the self-propulsion.

The general protocol for each simulation is the same: the colloids are randomly placed in the box, a magnetic field $\mathbf{B} = B_0\mathbf{e}_x$ may be applied for a duration of t_B before being turned off, and the colloids are left to move freely during 19τ. Only three parameters may vary across the simulations: the self-propulsion velocity v_0 and the magnetic dipole moment amplitude μ of the active dipoles, and the duration t_B during which the magnetic field is turned on. The magnitude of the external magnetic field is kept constant throughout simulations with $B' = 70$.

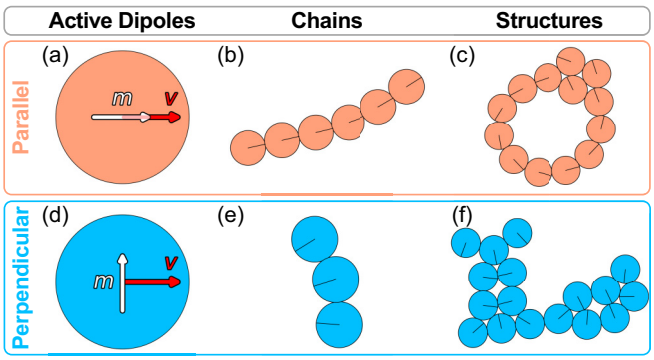

FIG. 1. Representation of (a) parallel and (d) perpendicular active dipoles. The orientation of each particle, and therefore the direction of the self-propulsion, is represented by the internal black line of each disk. Parallel active dipoles form (b) chains moving along their direction, that may collapse in (c) rotating spirals. Perpendicular active dipoles form (e) small chains moving perpendicularly to their longitudinal axis, that may collapse in (f) clusters.

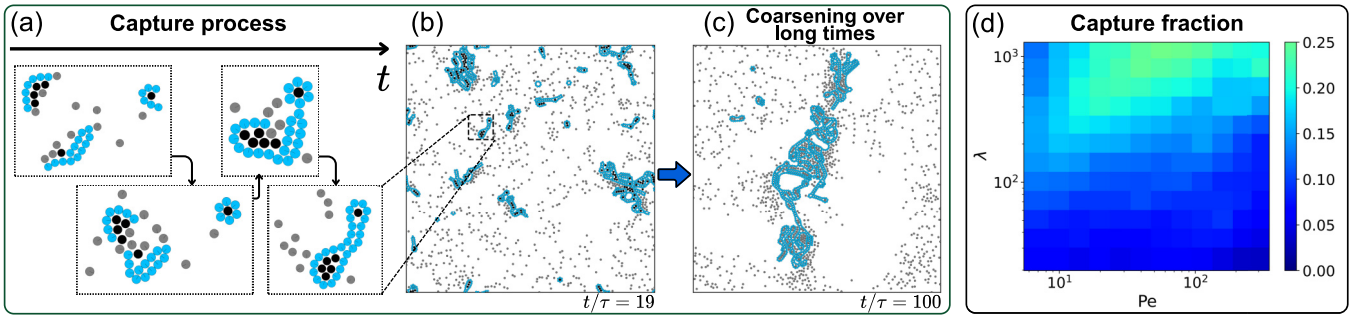

FIG. 2. (a) Various snapshots illustrating the evolution of structures formed by the active dipoles (colored in blue) over time, with passive colloids colored in gray if free and black if captured at the end of the process. (b) Final snapshot of the simulation for which the capture fraction is 0.148. (c) Coarsening of active structures after long times. (d) Capture fraction histogram depending on adimensional numbers Pe and λ. Each data point is averaged over 20 simulations.

In order to reduce the computational time required for these simulations, each colloid is linked to a square cell in the 2D space to only consider contacts and dipolar interactions with other particles already determined to be potential neighbors. While having no impact on the results for the calculation of contacts, since the cut off for WCA potential is at $2^{1/6}\sigma$, this cut off has an impact on the dynamics resulting from dipole-dipole interactions. A compromise between accuracy and efficiency was chosen to set the size of the cells to always consider dipole-dipole interactions up to 1/100th of the maximum interaction between touching colloids with aligned dipoles.

B. Structures of active dipoles

Active dipoles have a tendency to form chains of particles wandering through the 2D space. If the dipolar interactions are strong enough compared to the Brownian noise, these structures are stable until a perturbation makes the chain collapse on themselves. This perturbation is usually caused by the collision with active dipoles, especially with higher packing fractions of particles.

These phenomena happen whether the dipoles are oriented parallel or perpendicular to the propulsion. However, the way active dipoles are organized inside these structures is different, which leads to additional ways to cause the collapse of the chains, as shown in Fig. 1.

On one hand, parallel active dipoles form chains that move along the direction of the dipoles [30,31]. When perturbed, these chains may form spinning spirals that can become chains again over time. Particles are rarely completely stopped in the low packing fraction systems, forming chains that evolve continuously in size and shape.

On the other hand, perpendicular dipoles may form chains moving perpendicularly to their longitudinal axis. However, these structures are less stable compared to chains of active particles with parallel dipoles. They will quickly form clusters with other chains and particles, which are extremely stable comparatively. With time, such structures may grow bigger

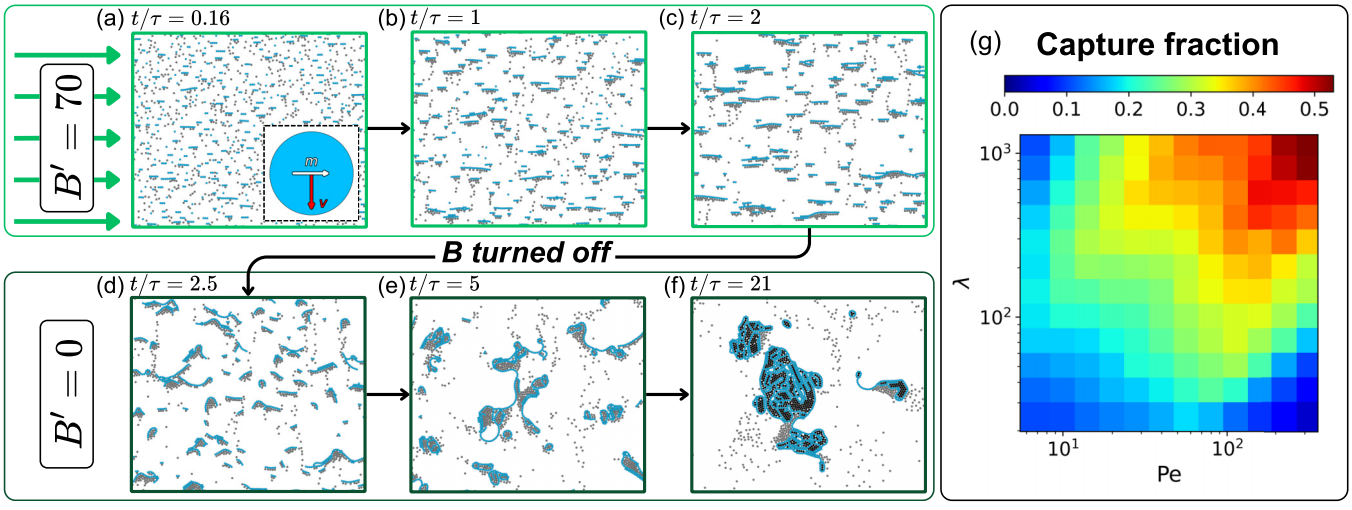

FIG. 3. Representation of the capture of passive particles by dipolar active particles with a magnetic field, with Pe = 68, λ = 283, $B' = 70$, and $\phi_a = \phi_p = 0.05$. (a)–(c) Chains of active dipoles growing with time passing, sweeping passive particles. (a) Active dipoles have their dipole (white) aligning with the magnetic field, forcing their orientation to self-propel downwards (red). (d)–(f) Once the magnetic field is turned off, chains bend and fuse while capturing passive colloids in bigger structures. (f) Final snapshot of a simulation with captured passive colloids in black, leading to a capture fraction of 0.571. (g) Capture fraction histogram depending on adimensional numbers Pe and λ, after a uniform magnetic field is turned on for a duration $t_B = \tau$. Each data point is averaged over 20 simulations.

and more passive, because the propulsion of the colloids tend to cancel each other out.

C. Trapping with active dipoles

Creating dense phases of passive colloids is possible through MIPS in mixtures of active and passive colloids. Yet this phenomenon is only observed at relatively high packing fractions [39,40]. Using perpendicular active dipoles instead of nonmagnetic active colloids may be a solution to form these dense phases of passive particles due to the collective behavior of these specific active dipoles.

Indeed, perpendicular active dipoles may collapse on each other due to collision with each other, but also by colliding with passive particles. Due to their ability to form small chains moving perpendicularly to their longitudinal axis, active dipoles can collect passive particles and trap them once they collide with other actives particles or chains. This leads to some passive particles being trapped in clusters formed by active dipoles, illustrated in Fig. 2.

These small structures also have a tendency to rearrange and fuse with each other, organizing as multiple layers of active dipoles pushing each other. Over time, they grow and coarsen by fusing with neighboring clusters, becoming less active as a whole and reducing the frequency of these events, until only big passive structures remain, as can be seen in Fig. 2(c). These bigger structures present a lot of defects due to the interplay between the activity and dipolar interactions

The efficiency of such a protocol is presented in Fig. 2(d). The capture fraction is the fraction of passive particles captured inside a structure of active dipoles at the end of the protocol. Averaged over multiple simulations, it becomes a measure of the probability that passive particle is captured after such a process. It is measured by calculating the fraction of passive particles that are in a structure encircled by active dipoles, as highlighted in black in Fig. 2(b), and averaged over 20 simulations. This is determined numerically by imposing a constant velocity to all active particles in four successive and different directions while calculating the dynamics of the passive particles due to contacts. A passive particle is considered captured if it followed the movements of the active ones in all four directions.

In the range of values studied for the parameters Pe and λ, there seems to be a peak efficiency of 0.25 by having the strongest dipolar interactions possible, but a specific balance for the activity is required to maximize the capture. Nonetheless, a vast majority of the passive colloids are not stuck in dense phases, even in the best case. The chains quickly collapse by fusing with each other, and once they do, they are unable to capture more passive particles. We reach a state where only a few particles have been captured and structures of active passive particles have become inert.

D. Impact of magnetic field

One way to improve the efficiency of this protocol is to create more stable chains. This can be done by applying an external magnetic field. When this field is applied, an additional torque will affect each active dipole and they will collectively have a tendency to orient themselves in one direction. The

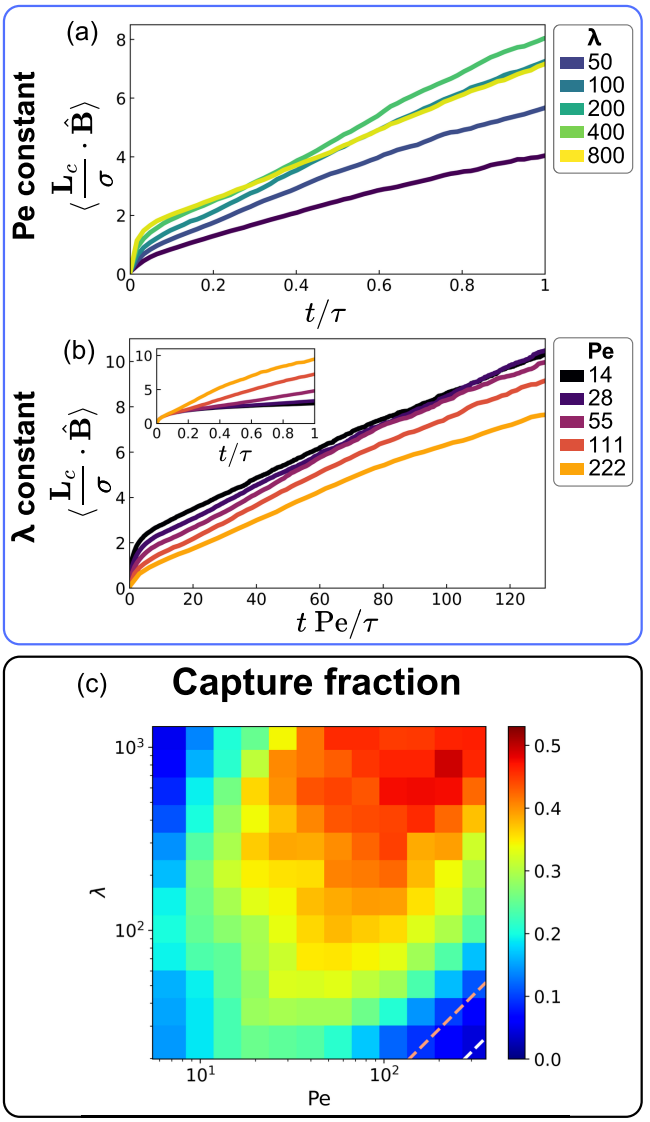

FIG. 4. (a) Evolution of the average length of chains $\mathbf{L}_c$ projected to magnetic field direction for different values of λ and fixed $\mathrm{Pe} = 96$. (b) Evolution of the average length of chains $\mathbf{L}_c$ projected to magnetic field direction over time rescaled by activity Pe for different values of Pe and fixed $\lambda = 200$, with the same data over time not rescaled by activity in the inset. (c) Capture fraction histogram depending on adimensional numbers Pe and λ, after a uniform magnetic field is turned on for a duration $t_B = \frac{136}{\mathrm{Pe}}\tau$. Each data point is averaged over 20 simulations. The white line represents the stability criterion (10) for $n = 1$ and the orange line for $n \to \infty$.

structures observed change over time, and are depicted in Fig. 3.

During the first phase, the magnetic field is turned on, leading to all active dipoles to orient themselves and propel in the same direction (a). They will also be attracted to other active dipoles next to them, since they have similar orientations, forming small chains. With time (b), (c), these chains grow bigger by fusing with others and start to sweep passive particles along the way. These horizontal chains continuously grow along their longitudinal axis and also create layered structures by encountering slower chains in front of them, as

seen in (c). After some time that depends on the characteristics of the active dipoles, the structures reach sizes comparable to the box, which causes unphysical simulations due to the periodic boundaries. We ensured that the external magnetic field was turned off before any chain could reach a size of half of the length of the box.

When the magnetic field is turned off (d), the active dipoles do not have the external orientational constraint, meaning that they will start to change shape and rotate due to noise and imbalance of self-propulsion across the structure. The chains will become more round and start to collide with each other, circling around passive colloids efficiently (e). This continuously happens until the structures get big enough so that they are mostly inert, and reach a final amount of particles captured (f).

The addition of this external magnetic field phase leads to a great increase in capture once it is turned off, as shown in Fig. 3(g). Comparing the results to the same simulations without magnetic field in Fig. 2(d), it becomes obvious that such protocol greatly improves capture in all cases, but especially for systems with high values of Pe and λ, for which capture fractions reach more than 0.5 on average.

By increasing λ, chains and structure grow bigger and are more stable, which is a positive contribution to the capture. And by increasing Pe, the active dipoles interact faster with the passive colloids, which also increases the number of passive colloids captured in the clusters in the same time frame.

Since the motivation for applying an external magnetic field is to favor the formation of longer chains, we can study how they grow for different values of Pe and λ. This can be achieved by analyzing the evolution over time of the average length $\mathbf{L}_c$ of each active dipole's chain projected on $\hat{\mathbf{B}}$, as shown in Fig. 4. By studying how λ affects this growth, we observe two distinct regimes over time in Fig. 4(a). First, for $t < 0.1\tau$, chains tend to grow quickly, and the growth depends monotonically on λ. This is the regime where the growth is primarily driven by the random initial configuration of the system, and particles being attracted to close neighbors, which is directly facilitated by stronger dipolar interactions. After this phase, chains are moving in the same direction and grow by fusing together. While stronger dipolar interactions allow active dipoles to be more attracted to each other when they are placed next to each other compared to their active direction, they are also more strongly repelled when following each other. Active chains become unable to grow by creating temporary structures of multiple layers then reorganize in a bigger chain. This can be seen in Fig. 4(a) as the growth is improved by increasing λ, until we reach higher values such as $\lambda = 800$ where the growth is hindered by dipolar interactions. In this case, activity is not strong enough to overcome the repulsion between chains following each other, and one of the ways for chains to grow is removed.

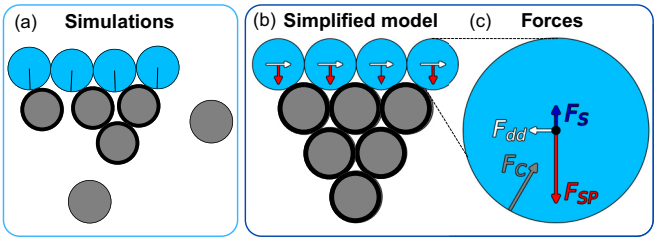

FIG. 5. (a) Illustration of a chain of active dipoles sweeping passive particles highlighted in black, while other passive particles are unaffected. (b) Simplest structure sweeping $n = 3$ layers of passive colloids while the magnetic field is on. (c) Illustration of the forces affecting the active dipole at the corner of the structure, which is susceptible to be pushed away from the structure due to contacts. The structure is stable if, for the active dipole on the edge of the chain, the force $F_{dd} \propto \lambda$ is greater than the force due to the contact with the passive colloid $F_c \propto \frac{n}{n+2}\mathrm{Pe}$.

By comparing how the average length of chains evolves over time for different values of Pe, as shown in the inset of Fig. 4(b), we also see two different behaviors for short and longer times. First, chains grow similarly, highlighting that this first growth regime is mainly due to active dipoles being attracted to close neighbors because of dipolar interactions. After 0.1τ, the chains grow differently depending on Pe, with faster active dipoles forming longer chains more quickly. Since chains are primarily growing by fusing with each other, activity facilitates it by making the chains explore more space in the same amount of time. With this understanding of the growth of chains in the second regime, we can understand whether activity simply accelerates the effects by studying how they grow if we rescale time with activity, as done in Fig. 4(b). We now see that the initial regime, where dipolar interactions dominate, differs since the scaling has been done compared to the activity. This induces a shift in value at shorter times, but we can also notice that chains grow at rates more similar to each other for longer times. Scaling the duration of the magnetic field to the activity by imposing $t_B \propto 1/\mathrm{Pe}$ allows us to reduce the correlated effects of time with Pe, and understand the effects of Pe and λ more directly on the capture process.

Figure 4(c) is an additional capture fraction histogram, for which the duration of the magnetic field is scaled to the activity ($t_B = \frac{136}{\mathrm{Pe}}\tau$). In this case, the specific regions of low and high capture fraction are seen to have been altered compared to Fig. 3(g).

For lower values of activity (Pe$<$50), capture fraction increases with Pe. Several phenomena could explain this, such as the increased relative importance of noise in low activity systems or the inability of chains to push passive particles. However, no definite conclusion can be made because another phenomenon affects the results: the duration of the relaxation phase after the magnetic field is turned off is not scaled to the activity. This results in capture fractions sometimes evaluated before structures become completely inert and unable to capture passive colloids.

For higher diffusive activity (Pe$>$50) and lower dipolar interactions ($\lambda < 300$), the capture fraction depends on both λ and Pe, with dipolar interactions improving the capture while activity hinders it. This suggests that the capture depends on a competition between both effects.

IV. DISCUSSION

The competition between activity and dipolar effects may happen in either of the two phases of the protocol, but is

more easily understandable when the magnetic field is turned on. An argument based on the stability of the most simple structure that sweeps passive particles can be made to evaluate this competition, as illustrated in Fig. 5. This structure is composed by a chain of $n+1$ active dipoles pushing $n(n+1)/2$ passive colloids organized on n layers. On one hand, the dipolar interactions are what is holding the structure together. On the other, the pyramid of passive particles are imposing forces that tend to break the chains through contacts the faster the structure is. The velocity of the structure can be evaluated to be $v_{\text{struct}} = \frac{2}{n+2} v_0$ by assuming that it is only determined by the self-propulsion of the active particles and the Stokes friction of all particles. The contact force felt by an active dipole at the edge of the structure can be recursively calculated to be $F_C = \frac{n}{\sqrt{3}} \gamma v_{\text{struct}}$. In the limit case for stability, all forces cancel out, and we obtain the relation $F_{dd} = \frac{n}{n+2} \frac{\gamma v_0}{\sqrt{3}}$ from the horizontal projection, with $F_{dd} = \frac{6k_B T}{\sigma} \lambda$ the dipolar force with the direct neighbor. Therefore, for such a structure to not decay into its equivalent of $n-1$ layers of passive colloids, we get the criterion

$$\lambda > \frac{\sqrt{3}}{12} \frac{n}{n+2} \text{Pe} \tag{10}$$

which gives a linear relation between λ and Pe. Two cases are of particular interest. If $n = 1$, this relation gives a criterion for the stability of a chain pushing a single passive colloid. It becomes $\lambda < \frac{\sqrt{3}}{36} \text{Pe}$ and indicates that no passive colloid can be captured through this sweeping mechanism. If $n \to \infty$, the relation indicates whether the dipolar interactions are strong enough to hold a structure of a pyramid of any number of layers or not. This becomes $\lambda > \frac{\sqrt{3}}{12} \text{Pe}$ and indicates that the structures will always stay stable during these sweeping phases. The relation (10) gives an idea on how the phenomena are driven through a competition between λ and Pe. These two cases are highlighted in Fig. 4(c). While explaining under which condition significant capture becomes possible, this reasoning only gives an intuition on how both effects contribute to the actual capture, and not an explanation on how effective the capture is depending on Pe and λ.

Thanks to the insights obtained from relation (10), we can investigate to what extent Pe and λ have separate effects on the capture, and how much we can describe the system by λ/Pe. This is explored in Fig. 6 by analyzing the system for different values of λ and Pe that keep the ratio λ/Pe constant. Regarding the chain growth in Fig. 6(a), we can see that compared to the case of fixed Pe or fixed λ in Fig. 4(b), keeping λ/Pe constant makes the growth over time collapse for the different values of (Pe; λ). This shows that the first growth regime for the chains does not exclusively depend on λ, but actually on λ/Pe. This longer time behavior is still correctly rescaled by the activity, meaning that all growth regimes exhibit similar behavior thanks to the scaling of time by Pe, even for low values of Pe where capture already decreases in Fig. 4(c).

Another aspect of the system that can be studied while the external magnetic field is turned on is the fraction of passive particles being swept by active chains. An example of swept passive particles is illustrated in Fig. 5(a) by particles highlighted in black. It is determined numerically by evaluating the number of passive particles moving with active dipoles

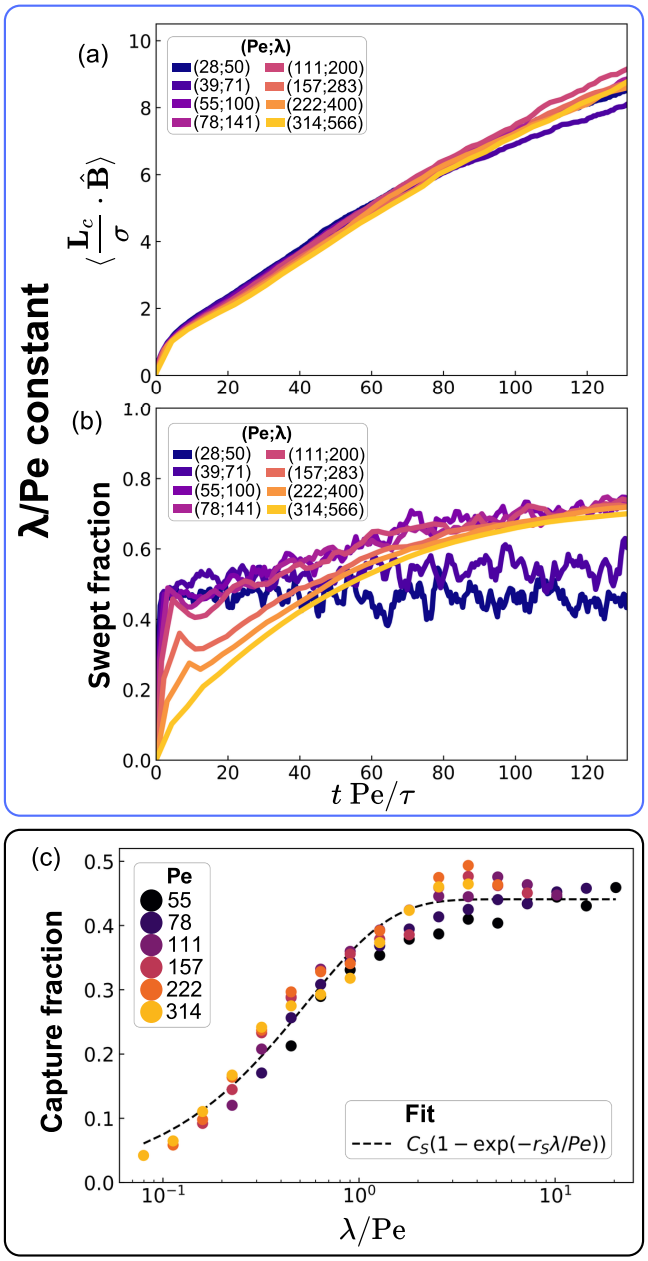

FIG. 6. Analysis of the system focusing on λ/Pe. Evolution of the (a) average length of chains and (b) fraction of passive particles swept (as illustrated in Fig. 5) over time rescaled by activity, for different activities Pe and dipole strength λ with $\lambda/\text{Pe} = 2.08$. (c) Capture fraction of passive colloids depending on λ/Pe in log scale for Pe >50, and fit to the saturating function $C(\frac{\lambda}{\text{Pe}}) = C_s(1 - \exp(-r_s \frac{\lambda}{\text{Pe}}))$ with $C_s = 0.441$ and $r_s = 1.853$.

inside clusters over the total amount of passive particles. This is plotted in Fig. 6(b), and two important pieces of information can be gleaned from it. First, the sweeping effect over time is not linearly linked to activity by a simple rescaling by Pe. However, we see that after this initial regime that depends on λ/Pe, the sweeping fraction converges to a similar curve for most of the values of (Pe; λ). Second, the curves that do not converge to the others are reaching a plateau with a lower sweeping fraction quickly, and are associated to low values of

activity. This implies that, beyond the possible undervaluation of capture fractions by evaluating the capture fraction before the process is finished, low Pe does affect the process of capture and a minimal value of Pe is required to do it most efficiently.

Analyzing the capture fraction depending on λ/Pe, illustrated in Fig. 6(c), also makes it visually clear that variations of Pe and λ do not affect the results significantly if their ratio is kept constant when Pe is sufficiently big, and that the capture process saturates. By fitting to a saturating exponential function of the form $C_s(1-\exp(-r_s\frac{\lambda}{\mathrm{Pe}}))$, we obtain values for the maximum capture C_s and the characteristic rate r_s. Both parameters are then constant for Pe and λ, but may depend on other parameters of the system which were kept fixed in this study.

V. CONCLUSION

Finding ways to control passive particles without any other characteristics than steric repulsion may be challenging, especially at low packing fractions [39,40]. External agents, through their activity and other properties, are one way of achieving this objective [53,54]. As seen in this case, complex active dipolar particles may act as sweeping agents for the passive colloids, but the sweeping and capture are done efficiently only if the dipoles are perpendicular to the self-propulsion direction.

While active perpendicular dipoles placed randomly are able to create dense phases of passive colloids through this sweeping effect, the efficiency can be further improved thanks to protocols of external magnetic fields applied globally to the system. A simple temporary activation of external magnetic field is enough to greatly increase the sweeping of passive colloids and their capture in dense phases.

To further improve this capture, an analysis about how the active and dipolar properties of the active dipoles influence the capture allows us to understand that dipolar interactions favor this effect, while the activity disfavors it, reaching a saturating plateau after a critical value of λ/Pe. However, lowering the activity also increases the time scale for which these effects are observed, preventing us to conclude on the all phenomena happening for $\mathrm{Pe} < 50$. This still allows us to find an optimal region of parameters λ and Pe that maximizes the capture.

Studying such a mixture of active dipoles and passive particles in 3D would not directly lead to a similar capture of passive particles, because the active dipoles would still only form moving strings [34]. To induce the self-assembly of moving 2D planes in 3D, more complex active particles would need to be designed and studied, for example by replacing the dipoles of active particles by quadrupoles.

ACKNOWLEDGMENTS

This work is financially supported by the University of Liège through the CESAM Research Unit.

DATA AVAILABILITY

The data that support the findings of this article are openly available [56].

[1] J. Elgeti, R. G. Winkler, and G. Gompper, Physics of microswimmers—single particle motion and collective behavior: a review, Rep. Prog. Phys. **78**, 056601 (2015).
[2] T. Vicsek and A. Zafeiris, Collective motion, Phys. Rep. **517**, 71 (2012).
[3] C. Dombrowski, L. Cisneros, S. Chatkaew, R. E. Goldstein, and J. O. Kessler, Self-concentration and large-scale coherence in bacterial dynamics, Phys. Rev. Lett. **93**, 098103 (2004).
[4] A. Sokolov, I. S. Aranson, J. O. Kessler, and R. E. Goldstein, Concentration dependence of the collective dynamics of swimming bacteria, Phys. Rev. Lett. **98**, 158102 (2007).
[5] A. Cavagna and I. Giardina, Bird flocks as condensed matter, Annu. Rev. Condens. Matter Phys. **5**, 183 (2014).
[6] A. Kudrolli, G. Lumay, D. Volfson, and L. S. Tsimring, Swarming and swirling in self-propelled polar granular rods, Phys. Rev. Lett. **100**, 058001 (2008).
[7] J. Deseigne, O. Dauchot, and H. Chaté, Collective motion of vibrated polar disks, Phys. Rev. Lett. **105**, 098001 (2010).
[8] A. Walther and A. H. E. Müller, Janus particles: Synthesis, self-assembly, physical properties, and applications, Chem. Rev. **113**, 5194 (2013).
[9] C. Bechinger, R. Di Leonardo, H. Löwen, C. Reichhardt, G. Volpe, and G. Volpe, Active particles in complex and crowded environments, Rev. Mod. Phys. **88**, 045006 (2016).
[10] S. A. Mallory, C. Valeriani, and A. Cacciuto, An active approach to colloidal self-assembly, Annu. Rev. Phys. Chem. **69**, 59 (2018).
[11] A. P. Solon, M. E. Cates, and J. Tailleur, Active brownian particles and run-and-tumble particles: A comparative study, Eur. Phys. J.: Spec. Top. **224**, 1231 (2015).
[12] D. Martin, J. O'Byrne, M. E. Cates, É. Fodor, C. Nardini, J. Tailleur, and F. Van Wijland, Statistical mechanics of active Ornstein-Uhlenbeck particles, Phys. Rev. E **103**, 032607 (2021).
[13] M. E. Cates and J. Tailleur, Motility-induced phase separation, Annu. Rev. Condens. Matter Phys. **6**, 219 (2015).
[14] Y. Fily and M. C. Marchetti, Athermal phase separation of self-propelled particles with no alignment, Phys. Rev. Lett. **108**, 235702 (2012).
[15] G. S. Redner, M. F. Hagan, and A. Baskaran, Structure and dynamics of a phase-separating active colloidal fluid, Phys. Rev. Lett. **110**, 055701 (2013).
[16] J. Bialké, H. Löwen, and T. Speck, Microscopic theory for the phase separation of self-propelled repulsive disks, EPL (Europhysics Letters) **103**, 30008 (2013).
[17] A. Suma, G. Gonnella, D. Marenduzzo, and E. Orlandini, Motility-induced phase separation in an active dumbbell fluid, EPL (Europhysics Letters) **108**, 56004 (2014).
[18] X.-q. Shi and H. Chaté, Self-propelled rods: Linking alignment-dominated and repulsion-dominated active matter, arXiv:1807.00294.
[19] O. Pohl and H. Stark, Dynamic clustering and chemotactic collapse of self-phoretic active particles, Phys. Rev. Lett. **112**, 238303 (2014).

[20] B. Liebchen, D. Marenduzzo, and M. E. Cates, Phoretic interactions generically induce dynamic clusters and wave patterns in active colloids, Phys. Rev. Lett. **118**, 268001 (2017).
[21] H. Stark, Artificial chemotaxis of self-phoretic active colloids: Collective behavior, Acc. Chem. Res. **51**, 2681 (2018).
[22] T. Vicsek, A. Czirók, E. Ben-Jacob, I. Cohen, and O. Shochet, Novel type of phase transition in a system of self-driven particles, Phys. Rev. Lett. **75**, 1226 (1995).
[23] J. Barré, R. Chétrite, M. Muratori, and F. Peruani, Motility-induced phase separation of active particles in the presence of velocity alignment, J. Stat. Phys. **158**, 589 (2015).
[24] A. Martín-Gómez, D. Levis, A. Díaz-Guilera, and I. Pagonabarraga, Collective motion of active Brownian particles with polar alignment, Soft Matter **14**, 2610 (2018).
[25] P. Baconnier, O. Dauchot, V. Démery, G. Düring, S. Henkes, C. Huepe, and A. Shee, Self-aligning polar active matter, Rev. Mod. Phys. **97**, 015007 (2025).
[26] M. Musacchio, A. P. Antonov, H. Löwen, and L. Caprini, Self-alignment and anti-self-alignment suppress motility-induced phase separation in active systems, J. Chem. Phys. **162**, 244902 (2025).
[27] S. H. L. Klapp, Collective dynamics of dipolar and multipolar colloids: From passive to active systems, Curr. Opin. Colloid Interface Sci. **21**, 76 (2016).
[28] A. Kaiser, K. Popowa, and H. Löwen, Active dipole clusters: From helical motion to fission, Phys. Rev. E **92**, 012301 (2015).
[29] J. Yan, M. Han, J. Zhang, C. Xu, E. Luijten, and S. Granick, Reconfiguring active particles by electrostatic imbalance, Nat. Mater. **15**, 1095 (2016).
[30] G.-J. Liao, C. K. Hall, and S. H. L. Klapp, Dynamical self-assembly of dipolar active Brownian particles in two dimensions, Soft Matter **16**, 2208 (2020).
[31] V. Telezki and S. Klumpp, Simulations of structure formation by confined dipolar active particles, Soft Matter **16**, 10537 (2020).
[32] M. Kelidou, M. Fazelzadeh, B. Parage, M. Van Dijk, T. Hooijschuur, and S. Jabbari-Farouji, Active string fluids and gels formed by dipolar active Brownian particles in 3D, J. Chem. Phys. **161**, 104904 (2024).
[33] A. B. Yener and S. H. L. Klapp, Self-assembly of three-dimensional ensembles of magnetic particles with laterally shifted dipoles, Soft Matter **12**, 2066 (2016).
[34] X. Chao, K. Skipper, C. P. Royall, S. Henkes, and T. B. Liverpool, Traveling strings of active dipolar colloids, Phys. Rev. Lett. **134**, 018302 (2025).
[35] G.-J. Liao and S. H. L. Klapp, Emergent vortices and phase separation in systems of chiral active particles with dipolar interactions, Soft Matter **17**, 6833 (2021).
[36] V. Telezki and S. Klumpp, Patterns of active dipolar particles in external magnetic fields, Phys. Rev. E **112**, 065422 (2025).
[37] B. Parage and S. Jabbari-Farouji, Modulation of nonequilibrium structures of active dipolar particles by an external field, Phys. Rev. E **112**, 065402 (2025).
[38] T. Kolb and D. Klotsa, Active binary mixtures of fast and slow hard spheres, Soft Matter **16**, 1967 (2020).
[39] J. Stenhammar, R. Wittkowski, D. Marenduzzo, and M. E. Cates, Activity-induced phase separation and self-assembly in mixtures of active and passive particles, Phys. Rev. Lett. **114**, 018301 (2015).
[40] R. Wittkowski, J. Stenhammar, and M. E. Cates, Nonequilibrium dynamics of mixtures of active and passive colloidal particles, New J. Phys. **19**, 105003 (2017).
[41] P. Dolai, A. Simha, and S. Mishra, Phase separation in binary mixtures of active and passive particles, Soft Matter **14**, 6137 (2018).
[42] D. Rogel Rodriguez, F. Alarcon, R. Martinez, J. Ramírez, and C. Valeriani, Phase behaviour and dynamical features of a two-dimensional binary mixture of active/passive spherical particles, Soft Matter **16**, 1162 (2020).
[43] S. Gokhale, J. Li, A. Solon, J. Gore, and N. Fakhri, Dynamic clustering of passive colloids in dense suspensions of motile bacteria, Phys. Rev. E **105**, 054605 (2022).
[44] M. Mijalkov and G. Volpe, Sorting of chiral microswimmers, Soft Matter **9**, 6376 (2013).
[45] B.-Q. Ai, S. Quan, and F.-g. Li, Spontaneous demixing of chiral active mixtures in motility-induced phase separation, New J. Phys. **25**, 063025 (2023).
[46] S. R. McCandlish, A. Baskaran, and M. F. Hagan, Spontaneous segregation of self-propelled particles with different motilities, Soft Matter **8**, 2527 (2012).
[47] J. Agudo-Canalejo and R. Golestanian, Active phase separation in mixtures of chemically interacting particles, Phys. Rev. Lett. **123**, 018101 (2019).
[48] J. Stürmer, M. Seyrich, and H. Stark, Chemotaxis in a binary mixture of active and passive particles, J. Chem. Phys. **150**, 214901 (2019).
[49] R. C. Maloney and C. K. Hall, Clustering and phase separation in mixtures of dipolar and active particles in an external field, Langmuir **36**, 6378 (2020).
[50] R. C. Maloney, G.-J. Liao, S. H. L. Klapp, and C. K. Hall, Clustering and phase separation in mixtures of dipolar and active particles, Soft Matter **16**, 3779 (2020).
[51] Y. Xi, T. Marzin, R. B. Huang, T. J. Jones, and P.-T. Brun, Emergent behaviors of buckling-driven elasto-active structures, Proc. Natl. Acad. Sci. **121**, e2410654121 (2024).
[52] R. Sinaasappel, K. R. Prathyusha, H. Tuazon, E. Mirzahossein, P. Illien, S. Bhamla, and A. Deblais, Particle sweeping and collection by active and living filaments, Phys. Rev. X **16**, 011003 (2026).
[53] W. Gao, X. Feng, A. Pei, Y. Gu, J. Li, and J. Wang, Seawater-driven magnesium based Janus micromotors for environmental remediation, Nanoscale **5**, 4696 (2013).
[54] B. Jurado-Sánchez, S. Sattayasamitsathit, W. Gao, L. Santos, Y. Fedorak, V. V. Singh, J. Orozco, M. Galarnyk, and J. Wang, Self-propelled activated carbon janus micromotors for efficient water purification, Small **11**, 499 (2015).
[55] M. E. O'Neill, PCG: A family of simple fast space-efficient statistically good algorithms for random number generation, Tech. Rep. No. HMC-CS-2014-0905 (Harvey Mudd College, Claremont, CA, 2014).
[56] A. Compagnie, N. Vandewalle, and E. Opsomer, Magnetically assisted trapping of passive colloids by active dipolar chains - data [Dataset], Zenodo, 2026, https://doi.org/10.5281/zenodo.17279856.